

Vector spin modeling for magnetic tunnel junctions with voltage dependent effects

Cite as: J. Appl. Phys. **115**, 17B754 (2014); <https://doi.org/10.1063/1.4868495>

Submitted: 22 September 2013 . Accepted: 17 December 2013 . Published Online: 14 April 2014

Sasikanth Manipatruni, Dmitri E. Nikonov, and Ian A. Young



View Online



Export Citation



CrossMark

ARTICLES YOU MAY BE INTERESTED IN

[Spin transfer torque devices utilizing the giant spin Hall effect of tungsten](#)

Applied Physics Letters **101**, 122404 (2012); <https://doi.org/10.1063/1.4753947>

[Perpendicular spin transfer torque magnetic random access memories with high spin torque efficiency and thermal stability for embedded applications \(invited\)](#)

Journal of Applied Physics **115**, 172615 (2014); <https://doi.org/10.1063/1.4870917>

[Spin-orbit torque magnetization switching of a three-terminal perpendicular magnetic tunnel junction](#)

Applied Physics Letters **104**, 042406 (2014); <https://doi.org/10.1063/1.4863407>

Applied Physics Reviews
Now accepting original research

2017 Journal
Impact Factor:
12.894

Vector spin modeling for magnetic tunnel junctions with voltage dependent effects

Sasikanth Manipatruni,^{a)} Dmitri E. Nikonov, and Ian A. Young

Exploratory Integrated Circuits, Components Research, Intel Corp., Hillsboro, Oregon 97124, USA

(Presented 6 November 2013; received 22 September 2013; accepted 17 December 2013; published online 14 April 2014)

Integration and co-design of CMOS and spin transfer devices requires accurate vector spin conduction modeling of magnetic tunnel junction (MTJ) devices. A physically realistic model of the MTJ should comprehend the spin torque dynamics of nanomagnet interacting with an injected vector spin current and the voltage dependent spin torque. Vector spin modeling allows for calculation of 3 component spin currents and potentials along with the charge currents/potentials in non-collinear magnetic systems. Here, we show 4-component vector spin conduction modeling of magnetic tunnel junction devices coupled with spin transfer torque in the nanomagnet. Nanomagnet dynamics, voltage dependent spin transport, and thermal noise are comprehended in a self-consistent fashion. We show comparison of the model with experimental magnetoresistance (MR) of MTJs and voltage degradation of MR with voltage. Proposed model enables MTJ circuit design that comprehends voltage dependent spin torque effects, switching error rates, spin degradation, and back hopping effects. © 2014 AIP Publishing LLC. [<http://dx.doi.org/10.1063/1.4868495>]

Integration of spin based memory and logic devices with CMOS offers an exciting opportunity to enhance the performance of modern computing systems.¹⁻³ In particular, on-chip embedded memory⁴ and non-volatile logic elements^{5,6} employing Magnetic Tunnel Junctions (MTJs) may enable ultra-low power, normally off and instantly on computing systems. However, close integration of MTJ with CMOS requires accurate circuit models, which comprehend the vector nature of spin torque driven dynamics,⁷ the intrinsic variability due to thermal noise,⁸ as well as the voltage dependent effects in MTJs.⁹⁻¹⁴ In this letter, we propose a vector circuit model for MTJs which comprehends the spin torque dynamics of the nanomagnet along with voltage dependent characteristics of the MTJs.

We propose a vector spin circuit model for MTJs based on 4-component spin conduction matrices which allows for calculation of vector spin current and spin torque. Vector spin circuit theory generalizes classical circuit theory to spin circuits by accurately relating the charge and spin currents ($\mathbf{I} = [I_c \ I_{sx} \ I_{sy} \ I_{sz}]$) with charge and spin voltage gradients ($\mathbf{V} = [\Delta V_c \ \Delta V_{sx} \ \Delta V_{sy} \ \Delta V_{sz}]$) in a circuit.¹⁵⁻¹⁷ A generic vector spin conductance (\mathbf{G} which relates \mathbf{I} and \mathbf{V}) comprises of 4×4 conductance elements relating the 4-component circuit variables.

We can make an equivalent vector spin circuit model for MTJ comprising two ferromagnet-to-oxide interfaces using conductance matrices. The vector spin equivalent circuit model for an MTJ is described in Figure 1. The model comprises of three nodes N0, N1, and N2. FM1 described by magnetization vector \hat{m}_1 is located between nodes N1 and N2. FM2 described by magnetization \hat{m}_2 is located between nodes N1 and N0. The 4-component conductivity of the FM1 and oxide interface is described by G_{FM1} and conductivity of the FM2 and oxide

interface is described by G_{FM2} . An effective conductivity G_{sf} can be used to describe the effect of spin scattering at the interface causing a transient noise or break down.¹⁸ The conductance matrix describing the spin transport across a FM/Oxide interface can be written as

$$\begin{bmatrix} I_c \\ I_{sx} \\ I_{sy} \\ I_{sz} \end{bmatrix} = \begin{bmatrix} G_{11} & \alpha(V_c)G_{11} & 0 & 0 \\ \alpha(V_c)G_{11} & G_{11} & 0 & 0 \\ 0 & 0 & G_{SL}(V_c) & G_{FL}(V_c) \\ 0 & 0 & -G_{FL}(V_c) & G_{SL}(V_c) \end{bmatrix} \begin{bmatrix} V_c \\ V_{sx} \\ V_{sy} \\ V_{sz} \end{bmatrix}, \quad (1)$$

where G_{11} is the interface conductivity (per interface) of the FM/MgO interface, $\alpha(V)$ is the spin polarization across the interface as a function of voltage, $G_{SL}(V_c)$ and $G_{FL}(V_c)$ are Slonczewski and field like torque contributions to the spin current across the interface [Appendix 1 of the supplementary material]. The voltage dependence of spin polarization $\alpha(V)$, $G_{SL}(V)$, $G_{FL}(V)$ is dependent on the detailed band structure of the electrodes and tunneling materials.^{15,19,20} The effect of magnetization rotation for a precessing MTJ can be described using the proposed model, where the 4 component conductances evolve as a function of the magnetization of the free magnet $G_{FM0}(\hat{m}) = R(\hat{m})^{-1}G_{FM0}(\hat{x})R(\hat{m})$, where R is a 4-component transformation to rotate the conductance matrices.^{16,17}

The proposed spin circuit model can accurately describe voltage dependent magneto-resistance (MR) of an MTJ. The voltage dependence in MR of an MTJ is attributed to the change in spin polarization associated with variations in the spin filtering effect of the MgO tunnel junctions.¹⁹ Figure 1(c) shows the voltage dependent magneto-resistance of an MTJ. Please see Appendix B of the supplementary material for a comparison with experiment. We show that the angular dependence of the magneto-resistance can be described using the proposed vector spin model for an MTJ. The

^{a)}Electronic mail: sasikanth.manipatruni@intel.com.

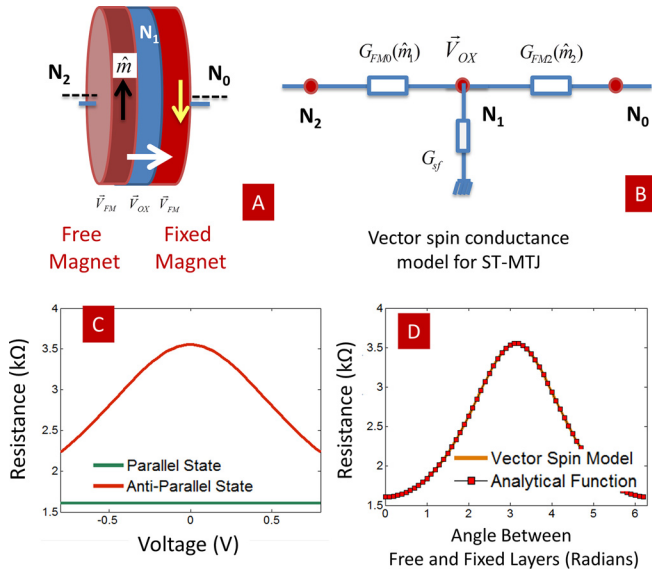


FIG. 1. (a) and (b) Vector spin conductance model for a Spin Torque Magnetic Tunnel Junction. The conductance of the FM/Oxide interface is dependent on the direction of magnetization. Magneto-resistance of a typical MTJ modeled with vector spin conduction model: (c) voltage dependent magneto-resistance, (d) angle dependent magneto-resistance compared with analytical function.

angular dependence of an MTJ follows:^{21,22} $G = G_p \cos^2 \frac{\theta}{2} + G_{ap} \sin^2 \frac{\theta}{2}$. The proposed model includes the effect of the non-collinear state of MTJ in the low resistance state allowing for calculation of loss of read margin in a MTJ.

A polynomial dependence of $\alpha(V)$ is assumed to obtain the accurate MR dependence with voltage and is described in Figure 2(a).

We show that the proposed model can capture the voltage induced effects in spin torque. Magnetic tunnel junctions exhibit both in-plane (τ_{SL}) and field like spin torque (τ_{FL}), unlike metallic spin valves.⁹⁻¹⁴ The voltage dependence of spin torque can play a critical role in the circuit behavior of MTJs especially in high speed transient conditions. In a 4-component model, the component G_{SL} contributes to the Slonczewski torque and G_{FL} contributes to the field like torque.¹⁵ As described by Butler *et al.*,⁹ the field like torque component (τ_{FL}) is usually an even parity function of voltage, whereas parallel component of spin torque (τ_{SL}) may exhibit wide range of non-monotonic behavior as a function of

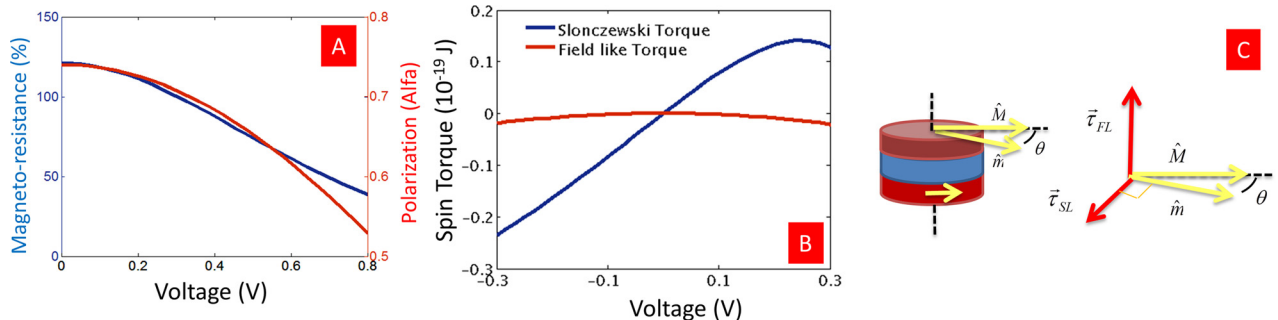


FIG. 2. Voltage effect on magneto-resistance and origin of the voltage dependent spin polarization of the tunneling electrodes in AP configuration: (a) Voltage effect on magneto-resistance captured by the change in interface spin polarization of the tunneling electrode. (b) Example voltage dependence of inplane and perpendicular components of spin torque in an MTJ. (c) Vector orientations of in-plane and field-like torque.

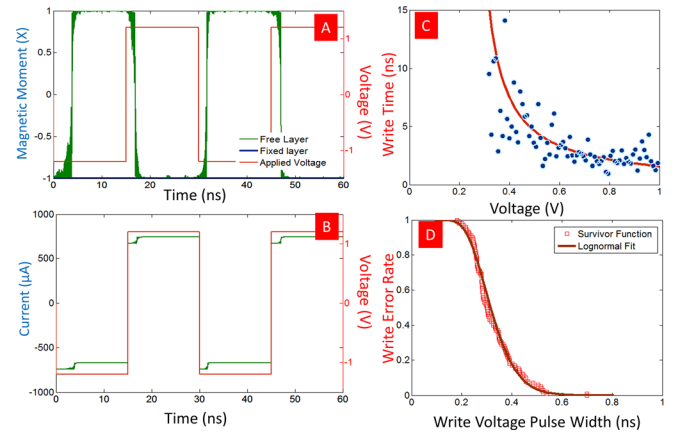


FIG. 3. Transient simulation of an MTJ with voltage dependent effects. (a) Magnetization dynamics of the free layer with thermal noise and voltage dependent models. (b) Applied voltage and current response. (c) Voltage dependent time response of the MTJ for AP-P transition, including thermal noise. (d) Write Error Rate of the MTJ for 1 V write pulse from AP-P.

applied voltage.¹² We phenomenologically describe the G_{SL} and G_{FL} as

$$G_{FL} = G_{11}g(V) \quad G_{SL} = G_{11}f(V), \quad (2)$$

where $f(V)$ and $g(V)$ are functions fitted to the voltage dependent torque measurements of magnetic tunnel junctions. Since $\tau_{FL} \propto G_{FL}V$ has an even parity, $g(V)$ has odd parity. In Figure 2(b), we show a possible configuration for field and in-plane torque.

The proposed model can be self-consistently coupled to the nanomagnet dynamics under the assumption that the spin torque effect is due to the absorption of the non-collinear injected spin into a nanomagnet.^{7,15}

$$\frac{\partial m}{\partial t} = -\gamma\mu_0[m \times \bar{H}_{eff}] + \alpha \left[m \times \frac{\partial m}{\partial t} \right] + \frac{1}{eN_s} \bar{I}_{s \perp m}(V, G), \quad (3)$$

where γ is the electron gyromagnetic ratio; μ_0 is the free space permeability; $\bar{H}_{eff}(T)$ is the effective magnetic field due to material/geometric/surface anisotropy, with the thermal noise component;²³ α_g is the Gilbert damping of the material, \bar{I}_{\perp} is the component of vector spin current perpendicular to the magnetization (\hat{m}), and N_s is the total number of Bohr magnetons per magnet. A coupled simulation of the

TABLE I. Calibration experiments for voltage dependent MTJ models.

Variables/trends to extract	Symbols	Experiment	E.g., References
TMR and polarization	$G_{11}, \alpha(V)$	DC MR	10
Polarization (V)	$\alpha(V)$	DC and AC MR	10
Field like torque	$G_{FL}(V)$	RF torkance	10, 11, 24, and 25
Slonczewski torque	$G_{SL}(V)$	RF torkance	10, 11, 24, and 25
Write time (V)	Cross check for $G_{FL}(V), G_{SL}(V)$	Pulsed IV	26
Write error rate	Cross check for $G_{FL}(V), G_{SL}(V)$	Pulsed IV	27

spin torque dynamics of an MTJ driven by the spin current response from a vector spin circuit model is shown in Figure 3(a). The effect of the rotation of the magnetization on the transport through the MTJ is captured by transforming the spin conductance matrix appropriately. Switching time versus an applied voltage pulse characteristics are shown in Figure 3(c). The proposed model can capture the effect of nanomagnet's thermal fluctuations. The proposed model also captures failure modes of the MTJ arising from thermally induced state change, thermal variability, and non-ideal features of the magneto-resistance and spin torque dynamics.²⁹

The elements of the MTJ model can be calibrated directly with experimentally measurable quantities. In Table I, we identify the basic set of calibration techniques to fit the voltage dependent conductance model in Figure 1 with the experimental behavior. Example quantitative and qualitative matches are shown in Appendix A of the supplementary material. G_{11} interface conductivity per interface can be matched to the observed resistance in the parallel state. The function $\alpha(V)$ is calibrated by comparing to DC and AC magneto-resistance measurements. Magnitudes of the in-plane ($\tau_{SL}(V)$) and field like spin torque ($\tau_{FL}(V)$) are matched to experiment via RF measurement of *spin torkance* in MTJs.^{24,25,28} Experiments for voltage vs. write pulse width²⁶ and voltage dependent write error rate²⁷ can improve the accuracy of the proposed models. A standard suite of experiments exists for extracting saturation magnetization (M_s), Gilbert damping (α_g), and magnetic anisotropy (H_k).⁵

In summary, we propose a vector spin circuit model for MTJs, which can capture the effects of nanomagnet dynamics combined with spin transport in non-collinear magnetic tunnel junctions. We show that the proposed model can capture: (a) DC Magneto-resistance and angular dependence of the nanomagnets on MTJ MR; (b) dynamic self-consistent treatment of the transport and LLG; (c) voltage effects on MR, in-plane, and perpendicular component of spin torque; (d) Thermal effects due to Langevin noise contributing to Write Error Rate; (e) Non-ideal MTJ behaviour, including asymmetric MR, back-hopping, and residual angle in the MTJ low resistance state. The proposed MTJ model can be

included in a standard version of the SPICE integrated circuit simulator via Spin circuit techniques.¹⁷ Supported by recent integration advances,^{4,5} close integration of magnetic devices could enable computing elements that complement/augment advanced CMOS technology for always connected, “normally off,” “instantly on” computers.

¹C. Chappert *et al.*, *Nature Mater.* **6**(11), 813–823 (2007).

²See <http://www.itrs.net/> for International Technology Roadmap for Semiconductors, Chapter PIDS, 2011.

³D. E. Nikonov and I. A. Young, *Technical Digest of the International Electron Devices Meeting (IEDM)*, 2012.

⁴H. Yoda *et al.*, *Technical Digest of the International Electron Devices Meeting (IEDM)*, 2012, p. 11.3.

⁵E. Kitagawa *et al.*, *Tech. Dig. Int. Electron Device Meet. 2012*, pp. 677–680.

⁶S. Manipatruni, D. E. Nikonov, and I. A. Young, *Appl. Phys. Lett.* **103**(6), 063503 (2013).

⁷J. Z. Sun, *Phys. Rev. B* **62**(1), 570 (2000).

⁸W. Butler *et al.*, *IEEE Trans. Magn.* **48**, 4684 (2012).

⁹I. Theodonis *et al.*, *Phys. Rev. Lett.* **97**(23), 237205 (2006).

¹⁰H. Kubota *et al.*, *Nat. Phys.* **4**, 37–41 (2008).

¹¹J. C. Sankey *et al.*, *Nat. Phys.* **4**(1), 67–71 (2008).

¹²M. Chshiev *et al.*, *IEEE Trans. Magn.* **44**(11), 2543–2546 (2008).

¹³C. Heiliger and M. D. Stiles, *Phys. Rev. Lett.* **100**(18), 186805 (2008).

¹⁴D. Datta *et al.*, *IEEE Trans. Nanotechnol.* **11**(2), 261–272 (2012).

¹⁵A. Brataas *et al.*, *Phys. Rep.* **427**(4), 157–255 (2006).

¹⁶S. Srinivasan, Ph.D. dissertation (Purdue University, 2012); S. Srinivasan *et al.*, *IEEE Trans. Magn.* **47**(10), 4026–4032 (2011).

¹⁷S. Manipatruni, D. E. Nikonov, and I. A. Young, *IEEE Trans. Circuits Syst.* **59**(12), 2801–2814 (2012).

¹⁸R. Stearrett *et al.*, *Appl. Phys. Lett.* **97**(24), 243502 (2010).

¹⁹W. H. Butler *et al.*, *Phys. Rev. B* **63**(5), 054416 (2001).

²⁰T. Z. Raza *et al.*, *J. Appl. Phys.* **109**(2), 023705 (2011).

²¹H. Jaffres *et al.*, *Phys. Rev. B* **64**(6), 064427 (2001).

²²F. Montaigne, C. Tiusan, and M. Hehn, *J. Appl. Phys.* **108**(6), 063912(2010).

²³W. F. Brown, *Phys. Rev.* **130**, 1677–1686 (1963).

²⁴S.-C. Oh *et al.*, *Nat. Phys.* **5**(12), 898–902 (2009).

²⁵C. Wang *et al.*, *Nat. Phys.* **7**(6), 496–501 (2011).

²⁶Z. M. Zeng *et al.*, *Appl. Phys. Lett.* **98**(7), 072512 (2011).

²⁷L. Kangho, J. J. Kan, E. E. Fullerton, and S. H. Kang, *IEEE Magn. Lett.* **3**, 2232906 (2012).

²⁸L. Xue *et al.*, *Appl. Phys. Lett.* **101**(2), 022417 (2012).

²⁹See supplementary material at <http://dx.doi.org/10.1063/1.4868495> for comparison to experimental work and description of the conductances G_{FL} and G_{SL} .